Aromatic congeners of bilirubin: synthesis, stereochemistry, glucuronidation and hepatic transport

Justin O. Brower,[a] David A. Lightner[a,*] and Antony F. McDonagh[b,*]

[a]Department of Chemistry, University of Nevada, Reno, NV 89557-0020, USA
[b]G.I. Unit and the Liver Center, University of California, San Francisco, CA 94143-0538, USA

Abstract—A new synthetic analog (**1**) of the bile pigment bilirubin-IXα (bilirubin, Fig. 1) with phenyl groups replacing vinyl was prepared by a constitutional scrambling reaction of a mixture of two new, symmetric phenylrubin analogs (**2** and **3**) of bilirubin-XIIIα and IIIα. The former (**2**) with two *endo*-phenyls, and the latter (**3**) with two *exo*-phenyls were synthesized by condensation of a dipyrrylmethane dialdehyde with appropriate methylphenylpyrrolinones, which were prepared in several steps from 4-methyl-3-phenyl-2-(*p*-toluenesulfonyl)pyrrole, obtained by the Barton–Zard pyrrole synthesis. Nuclear Overhauser effect ^{1}H NMR studies of **1**–**3** confirm that, like their bilirubin equivalents, these yellow-orange pigments adopt an intramolecularly hydrogen-bonded ridge–tile conformation. Reverse phase HPLC and TLC suggest that **3** is less polar than **2**, and that **1** has intermediate polarity. Large differences in the induced circular dichroism spectra of **1**–**3** were found in pH 7.4 aqueous buffered solutions of human serum albumin.

Despite the presence of bulky, lipophilic phenyl groups, **1**–**3** are metabolized like natural bilirubin in rats and require glucuronidation by the same enzyme for canalicular secretion from the liver into bile. However, there are striking qualitative differences between the three pigments in the ratio of mono- to diglucuronides formed. Phenyl substituents at the *exo* positions of the lactam rings diminish the proportion of diglucuronide more than phenyl substituents at the *endo* positions. © 2001 Elsevier Science Ltd. All rights reserved.

1. Introduction

Humans become jaundiced because of an inability to efficiently eliminate the yellow pigment, bilirubin (Fig. 1),[1,2] which is cytotoxic and a powerful anti-oxidant.[3]

Bilirubin is formed in large amounts in mammals but is not excreted in bile or urine to any significant degree.[4] For excretion, it is metabolized by a hepatic glucuronosyl transferase enzyme to isomeric monoglucuronides that are excreted into bile. Although there are several glucuronosyl
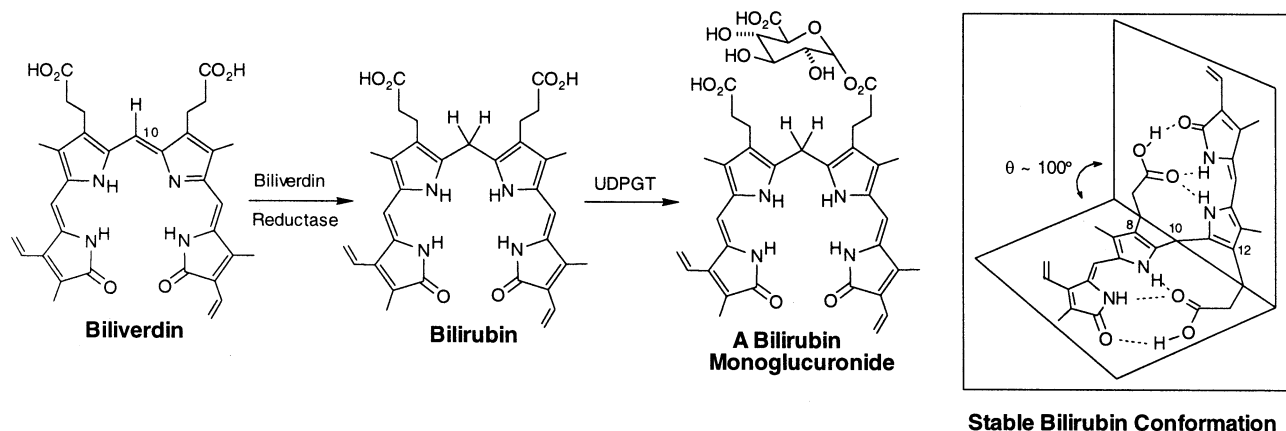

Figure 1. Enzymic conversion of (blue-green) biliverdin to (yellow-orange) bilirubin, and formation of a bilirubin mono-glucuronide. Formation of mono-glucuronides (and the diglucuronide) is an essential step in the hepatic elimination of bilirubin. The structures are drawn in a porphyrin-like shape, except for the inset, where bilirubin is shown in its most stable conformation: intramolecularly hydrogen-bonded and folded like a ridge–tile. Hydrogen bonds are shown by dashed lines.
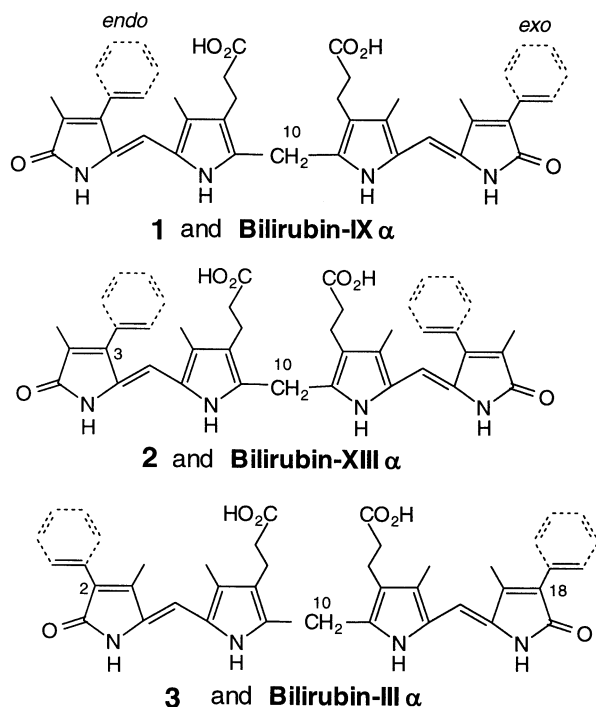
Figure 2. Linear representations of bilirubin IXα, IIIα and XIIIα (solid lines) and their analogs (**1–3**) with phenyls superimposed (dashed lines).

transferases in the liver, with frequent cross-reactivity for substrates, only a specific isozyme (UGT1A1) glucuronidates bilirubin in vivo in rats and humans.[1–3] This enzyme also accepts the two bilirubin monoglucuronides as substrates, so that bilirubin diglucuronide is excreted in bile along with the monoglucuronides. Presently little is known about the mechanism of glucuronidation or about the protein–pigment interactions at the catalytic site of the enzyme. The high selectivity of bilirubin for UGT1A1 and its double conjugation to a diglucuronide are unusual, and it is surprising that bilirubin, which is an organic anion at physiologic pH, should require glucuronidation for excretion into bile. Its metabolic precursor biliverdin, which is only two hydrogens different and has similar pK_as, can be eliminated rapidly from the liver into bile intact without undergoing conjugation.[4] This metabolic difference between the two pigments is apparently related to their lipophilicities, which are dependent on their three-dimensional structures. Biliverdin adopts lock–washer conformations, but bilirubin and its anions fold into ridge–tile shapes (Fig. 1) that are stabilized by a network of intramolecular hydrogen bonds.[5,6]

In a previous paper,[7] we reported the synthesis of lipophilic bilirubins in which the increased lipophilicity derived from *n*-butyl substituents. The presence of *n*-butyl groups at the 3 and 17 (*endo*) positions on the lactam rings did not have a large effect on glucuronidation and excretion. Biliary excretion was somewhat slower than for the corresponding ethyl substituted compound and the proportion of mono to diglucuronide formation was increased. *n*-Butyl groups at the 2 and 19 (*exo*) positions, adjacent to the lactam carbonyls, had a much larger effect. Biliary excretion was greatly retarded and only the monoglucuronide was detectable in bile. In the present work, we describe the syntheses of three

novel lipophilic bilirubins (**1–3**, Fig. 2) in which the enhanced lipophilicity stems from the replacement of vinyl groups with relatively bulky phenyl groups. These are the first bilirubins containing aromatic substituents. Despite their relative bulk, the phenyl substituents are not expected to alter the three-dimensional structure and hydrogen bonding depicted in Fig. 1, but their presence could hamper the access of pigment to the active site of UGT1A1.

2. Results and discussion

2.1. Syntheses

Preparation of the unsymmetric phenylrubin (**1**), the phenyl analog of the natural bilirubin (IXα, Fig. 2) required the syntheses (Scheme 1) of two symmetric phenylrubins (**2** and **3**), themselves phenyl analogs of the symmetric bilirubins-XIIIα and IIIα. The key synthetic step in the synthesis of **1** was an acid-catalyzed, constitutional isomerization scrambling reaction that had been developed and used successfully in other work.[8] For ease of chromatographic separation, the scrambling reaction was designed to mix a dimethyl ester and a diacid so as to produce the hybrid mono-methyl ester, which would be predicted to have polarity intermediate between the more polar diester and the less polar diacid and would thus be easily separated chromatographically. Consequently, dimethyl ester **5** was mixed and scrambled using acid catalysis with diacid **3** to produce mono-methyl ester **4** in a mixture that was easily separated by radial chromatography on silica gel.

The precursor symmetric phenylrubins **2** and **5** were prepared by piperidine-catalyzed condensation of 3-methyl-4-phenylpyrrolin-2-one (**6**) with the known 5,5′-diformyl-dipyrrylmethane **13**,[7,9,10] to give **5**, or with diacid **14** (derived from **13**) to give **2**. Similarly, symmetric phenylrubin **3** was prepared by reaction of 4-methyl-3-phenylpyrrolinone **7** with **14** to give **3**. Curiously, although condensation of **13** with **6** in refluxing methanolic sodium hydroxide also gave rubin product **2** in ~35% yield, the same reaction failed to convert a mixture of **13** and **7** to **3**.

The two pyrrolinones (**6** and **7**) were synthesized from a common monopyrrole precursor (**10**), which was prepared in 65% yield by a Barton–Zard pyrrole-forming reaction between *p*-toluenesulfonylmethyl isocyanide (TosMIC)[10] and 2-nitro-1-phenylpropanol acetate (**15**),[11] which was prepared from commercially available, inexpensive benzaldehyde and nitroethane. A similar Barton–Zard reaction to yield **11** directly from 3-nitro-3-phenyl-2-propanol acetate was less attractive because synthesis of the latter requires coupling sensitive α-nitrotoluene with acetaldehyde and because previous studies[11] had shown that **10** could be converted nearly completely into **11** by TFA-catalyzed isomerization. Isomerization of **10** smoothly led to an equilibrium mixture that favored **11** (10:1) and from which pure **11** could be isolated by fractional crystallization. Tosylpyrroles **10** and **11** could be converted to the desired pyrrolinones **6** and **7** by either of two routes. In one, pyrrolinone **8** was prepared from **10**, first by bromination (to give **12**), then by treatment with TFA and water. Applying this
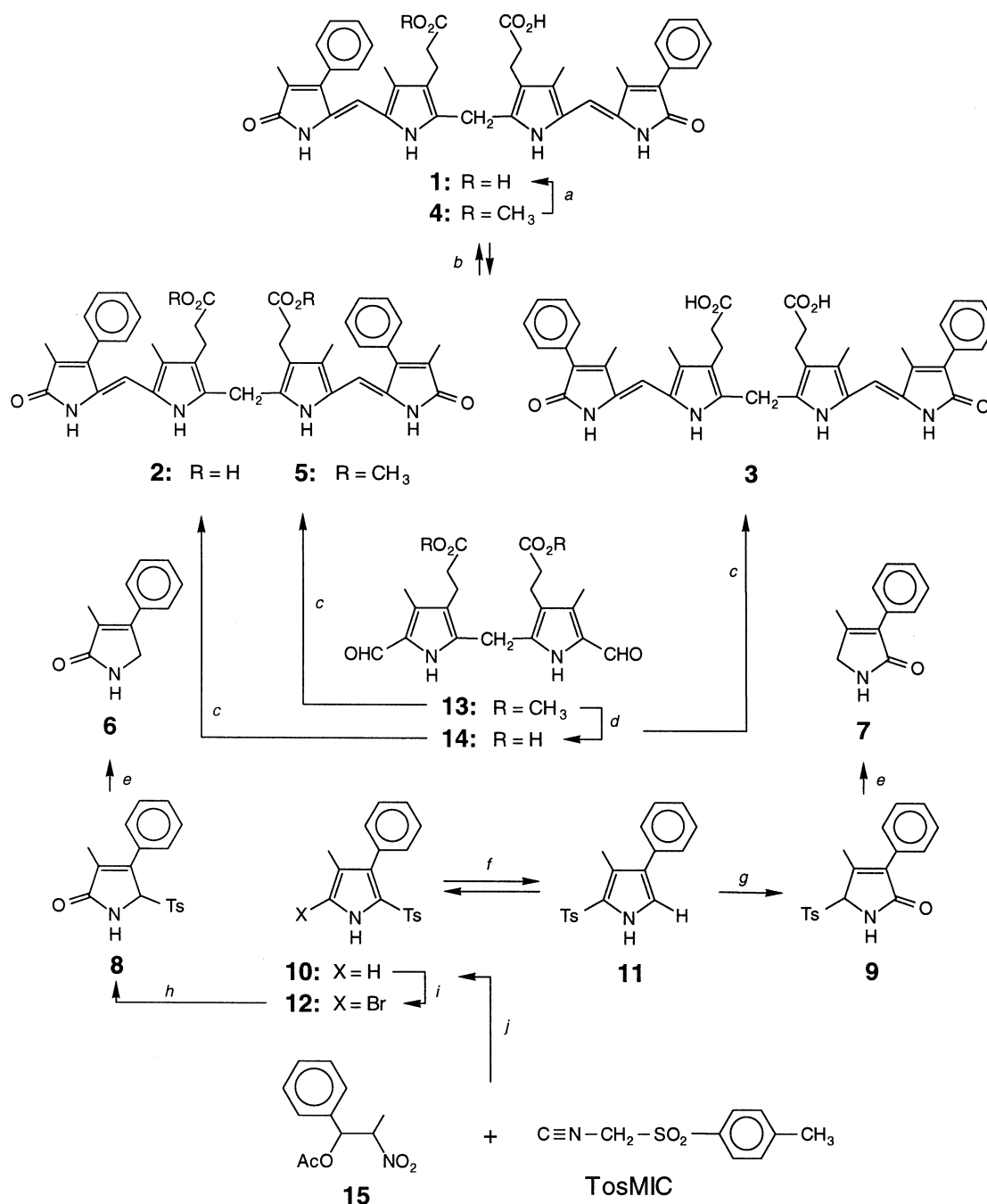
Scheme 1. [a]NaOH/CH$_3$OH–H$_2$O/refl., then HOAc; [b]DMSO/HCl; [c]piperidine; [d]6 M aq KOH–CH$_3$OH, then HCl; [e]NaBH$_4$/EtOH; [f]TFA/CH$_2$Cl$_2$ (1:9); [g]H$_2$O$_2$–HOAc; [h]TFA–H$_2$O (5:1); [i]PhNMe$_3^+$Br$_3^-$/CH$_2$Cl$_2$; [j]Guanidine/THF–iPrOH.
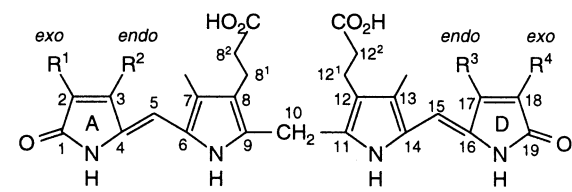
method for converting **11** to **9**, however, led to highly variable (1–50%) yields of **7**. In an alternate route, direct oxidation of **11** to **9** in 25% yield was achieved with H$_2$O$_2$ in HOAc. Removal of the tosyl group from either **8** or **9** proceeded smoothly and in high yield by reaction with NaBH$_4$ in CH$_3$OH to afford the desired pyrrolinones, **6** and **7**, respectively.

The central core dipyrrylmethane dialdehyde (**13**) had been prepared earlier[7,10] in three steps from methyl 3-[2-(carbo-*tert*-butoxy)-3-methyl-5-acetoxymethyl-1*H*-pyrrolyl]pro-pionate.[10] Saponification of diester **13** afforded diacid **14** in 90% yield.

2.2. Constitutional structure and conformations

Although the structures of **2** and **3** follow logically from their syntheses from well-characterized smaller molecules, and the structure of **1** follows from the structures of **2** and **3** and the well-studied constitutional scrambling reaction,[8] the structures were confirmed from their ^{13}C NMR spectra in (CD$_3$)$_2$SO (Table 1). For comparison purposes, we also show the collected ^{13}C NMR chemical shifts and assign-ments for bilirubins-IIIα, IXα and XIIIα. As might be expected, the resonances of the symmetric IIIα and XIIIα structures correlate with those observed in the IXα struc-ture. There is also a good correlation between the chemical

Table 1. Comparison of ^{13}C NMR chemical shift assignments of phenyl-bilirubin analogs **1** ($R^1=R^3=Me$, $R^2=R^4=Ph$), **2** ($R^1=R^4=Me$, $R^2=R^3=Ph$) and **3** ($R^1=R^4=Ph$, $R^2=R^3=Me$) with bilirubin-XIIIα ($R^1=R^4=Me$, $R^2=R^3=Vn$), bilirubin-IXα ($R^1=R^3=Me$, $R^2=R^4=Vn$) and bilirubin-IIIα ($R^1=R^4=Vn$, $R^2=R^3=Me$)

Position	Bis-phenyl bilirubin			Bilirubin		
	XIIIα (2)	IXα (1)	IIIα (3)	XIIIα	IXα	IIIα
COOH	173.93	173.89		173.91	173.94	
$8^3/12^3$		173.89	173.91		173.95	174.04
CO	171.31	171.30		171.09	171.09	
1/19		170.36	170.38		171.22	170.22
2/18	123.42	123.31		124.00	124.00	
		122.47	122.38		125.98	125.95
3/17	140.36	140.41		145.13	145.13	
		141.84	141.96		141.88	141.89
4/16	127.43	127.54		128.04	128.06	
		128.31	128.21		128.49	128.55
5/15	99.13	99.12		101.11	101.09	
		99.96	100.00		99.89	99.89
6/14	122.04	122.12		122.24	122.19	
		122.31	122.23		122.06	122.20
7/13	119.52	119.59		119.55	119.58	
		119.79	119.79		119.74	119.78
8/12	123.21	123.31		123.24	123.25	
		124.01	124.11		123.92	123.97
9/11	130.79	130.63		130.81	130.81	
		131.39	131.34		132.26	132.26
10-CH$_2$	23.58	23.60	23.67	23.74	23.65	23.74
CH$_3$ $2^1/3^1$ ($18^1/17^1$)	9.47	9.36		9.04	9.06	
		9.18	9.25		10.68	10.74
$3^1/2^1$ ($17^1/18^1$)	127.36	127.34		132.16	132.17	
		127.03	127.08		131.24	131.29
$2^2/3^2$ ($17^2/18^2$)	122.04	121.95		129.44	129.43	
		117.12	117.12		129.19	129.18
$2^1/3^1$ ($18^1/17^1$)	–	–	–	128.47	128.6	
	–	–	–		127.97	128.00
$2^4/3^4$ ($18^4/17^4$)	–	–	–	128.29	128.30	
	–	–	–		127.03	127.03
CH$_3$ $7^1/13^1$	9.12	9.10		9.00	9.02	
		9.10	9.13		9.15	9.20
CH$_2$ $8^1/12^1$	19.22	19.24		19.19	19.23	
		19.24	19.21		19.23	19.29
CH$_2$ $8^2/12^2$	34.21	34.28		34.17	34.20	
		34.28	34.17		34.20	34.26

Chemical shifts in δ (ppm) downfield from $(CH_3)_4Si$ for spectra run in $(CD_3)_2SO$ solvent. Assignments are made from multiple-bond H–C COSY experiments.

shifts of the phenylbilirubins and those of their vinyl analogs, especially the propionic acid carbons, the lactam CO, the methyl substituents and most of the ring carbons. Noticeable differences are found in C-2/18, C-9/11 and C-$3^1/17^1$ of **3** and bilirubin-XIIIα, and in C-3/17 and C-5/15 of **2** and mesobilirubin-XIIIα, which has ethyl groups in place of the phenyls of **2**. Corresponding differences in shielding are found in the IXα structures. It is interesting to note that while the $2^1/18^1$-CH$_3$ groups of the XIIIα isomers differ by only ~0.5 ppm, with those of **2** being more shielded, the $3^1/17^1$-CH$_3$ groups of the IIIα isomers differ by ~1.5 ppm, with **3** being more deshielded. These data suggest that the *endo*-phenyl rings of **2** lie perpen-

dicular to the lactam ring, thus exposing the neighboring $2^1/18^1$ methyls to the (shielding) face of the aromatic ring. On the other hand, the *exo*-phenyls of **3** are more likely to lie in the plane of the lactam, thereby exposing the neighboring $3^1/17^1$-CH$_3$ to the edge of the (deshielding) aromatic ring.

Consistent with the ^{13}C NMR results, in the ^{1}H NMR run in CDCl$_3$ (Table 2), the $3^1/17^1$-CH$_3$ groups are relatively more deshielded in **3** than in bilirubin-IIIα or **2**, and the $2^1/18^1$-CH$_3$ groups in **2** are relatively more shielded than in bilirubin-XIIIα or **3**. Consistent with an *endo*-phenyl conformation with the aromatic ring perpendicular to the lactam, the nearby 7/13-CH$_3$ of **2** is more shielded than that of **3**. In addition, the 5/15 =CH of **2** is more shielded than that of bilirubin-XIIIα or **3**, and the 5/15 =CH of **3** is more deshielded than that of bilirubin-IIIα. For most other chemical shifts, there are strong similarities, except for the obvious differences between phenyl and vinyl groups. Just as the signals for bilirubin-IXα are a composite of those from bilirubins-IIIα and XIIIα, so are the chemical shifts found in **1** a composite of those from **2** and **3**.
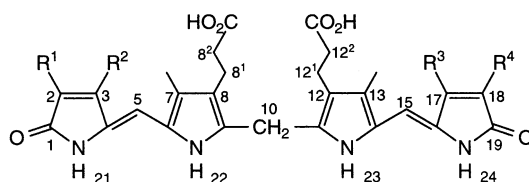
The COOH and NH chemical shifts have been shown to be characteristic of intramolecular hydrogen bonding of the type shown in Fig. 1 for natural bilirubin and its symmetric isomers. Those of phenylrubins **1**–**3** are very similar to those found in bilirubin-IIIα, IXα and XIIIα, which suggests intramolecular hydrogen bonding in similar ridge–tile conformations. In such conformations, the propionic acid segment is held in a fixed staggered geometry and exhibits a characteristic ABCX splitting pattern (CH$_A$H$_X$–CH$_B$H$_C$–CO$_2$H) rather than the A$_2$B$_2$ splitting pattern typically found where greater segmental motion is possible in the chain, as in $(CD_3)_2SO$ solvent.[7,12] The coupling constants observed (Table 3) confirm the fixed staggered geometry in the symmetric IIIα and XIIIα isomers. The coupling constant analysis in the IXα isomer is complicated by overlapping signals from the non-equivalent C(8) and C(12) propionic acids, but the patterns are clearly of the ABCX type.

Further confirmation of the intramolecularly hydrogen-bonded ridge–tile conformations of **1**–**3** may be found in NOE studies. Significant NOEs between the pyrrole and lactam NHs, and between the C(5/15)-H and the C(7/13)-CH$_3$ groups confirm the *syn-Z* dipyrrinone geometry (Fig. 3). Weaker NOEs between the COOH and lactam NH show a close proximity, characteristic of that found in Figs. 1 and 5, and in the crystal structure of bilirubin-IXα. As with the ordinary bilirubins and mesobilirubins with propionic acids at C(8) and C(12), molecular dynamic calculations reaffirm the intramolecularly hydrogen-bonded ridge–tile confor-mation (Fig. 4) as the global energy-minimum.[13]

2.3. UV–vis spectra

In bilirubin UV–vis spectra (Table 4) one of the features of λ^{max} for the long wavelength absorption is that *endo*-vinyls cause a hypsochromic shift; whereas *exo*-vinyls cause a bathochromic shift. This is clearly seen in comparing bilirubin-XIIIα and IIIα over a wide range of solvents and polarity. This same type of difference may also be seen for **2** and **3**, with *endo*-phenyls and *exo*-phenyls, respectively.

Table 2. Comparison of the ^{1}H NMR chemical shift assignments of phenyl rubins **1** (R^1,R^3=Me, R^2,R^4=Ph), **2** (R^1,R^4=Me, R^2,R^3=Ph) and **3** (R^1,R^4=Ph, R^3,R^2=Me) with bilirubin-IXα (BR-IX, R^1,R^3=Me, R^2,R^4=Vn), bilirubin-XIIIα (BR-XIII, R^1,R^4=Me, R^2,R^3=Vn) and bilirubin-IIIα (BR-III, R^1,R^4=Vn, R^2,R^3=Me) in CDCl$_3$

Position	Bis-phenyl bilirubin			Bilirubin		
	XIIIα (**2**)	IXα (**1**)	IIIα (**3**)	XIIIα	IXα	IIIα
$8^3/12^3$-COOH	13.69	13.74		13.67	13.68	
		13.62	13.66		13.68	13.71
21/24-NHCO	10.90	10.92		10.79	10.80	
		10.84	10.85		10.69	10.70
22/23-NH	9.28	9.30		9.26	9.27	
		9.35	9.36		9.29	9.30
2/3, 17/18-CH$_3$	2.03	2.02		1.99	1.99	
		2.27	2.27		2.18	2.18
$2^1/3^1$, $17^1/18^1$	–		–	6.61[a]	6.61	
					6.49	6.50[a]
$2^2/3^2$ $17^2/18^2$	7.29[b]	7.29		5.62[c]	5.62/5.37	5.37[c]
		7.47	7.47[b]	5.59[c]	5.59/5.35	5.35[d]
$2^3/3^3$, $17^3/18^3$	7.46[e]	7.46		–	–	–
		7.41	7.41[e]			
$2^4/3^4$, $17^4/18^4$	7.43[f]	7.43		–	–	–
		7.30	7.30[f]			
5,15-CH=	5.97	5.97		6.21	6.21	
		6.23	6.22		6.13	6.14
7,13-CH$_3$	1.91	1.92		2.16	2.16	
		2.21	2.20		2.15	2.15
$8^1,12^1$-CH$_2$	3.01[g,h]	3.01/3.04[g]	3.04[g,h]	3.02[g,h]	3.02[g]	3.01[g,h]
	2.56[g,h]	2.56/2.61[g]	2.60[g,h]	2.58[g,h]	2.58[g]	2.58[g,h]
$8^2,12^2$-CH$_2$	2.89[g,h]	2.89/2.93[g]	2.93[g,h]	2.90[g,h]	2.90[g]	2.90[g,h]
	2.79[g,h]	279/2.82[g]	2.82[g,h]	2.82[g,h]	2.90[g]	2.81[g,h]
10-CH$_2$	4.08	4.10	4.11	4.08	4.08	4.08

Chemical shifts in δ (ppm) downfield from (CH$_3$)$_4$Si.
[a] J=2.0, 11.5 Hz.
[b] d, J=7.5 Hz.
[c] dd, J=2.0, 17.5 Hz.
[d] J=14.0 Hz.
[e] t, J=7.5 Hz.
[f] d, J=7.5 Hz.
[g] Multiplets.
[h] See Table 3 for coupling constants.

Table 3. ^{1}H NMR chemical shifts and coupling constants for the propionic acid $-C_\beta H_A H_X - C_\alpha H_B H_C - CO_2 H$ segments of phenyl rubins **2** and **3** and bilirubin-XIIIα (BR-XIII) and bilirubin IIIα (BR-III) in CDCl$_3$ at 22°C

C(8,12)	β-CH$_2$		α-CH$_2$	
	H$_X$	H$_A$	H$_B$	H$_C$
δ	2.56	3.01	2.89	2.79
2	J_{BX}=1.5	J_{AB}=15.0	J_{AB}=13.0	J_{AC}=3.0
	J_{CX}=4.0	J_{AC}=3.0	J_{BX}=1.5	J_{CX}=4.0
	J_{AX}=−14.5	J_{AX}=−14.5	J_{BC}=−19.5	J_{BC}=−19.5
δ	2.6	3.04	2.93	2.82
3	J_{BX}=1.5	J_{AB}=13.5	J_{AB}=13.5	J_{AC}=3.0
	J_{CX}=4.5	J_{AC}=3.0	J_{BX}=1.5	J_{CX}=4.5
	J_{AX}=−14.5	J_{AX}=−14.5	J_{BC}=−15.8	J_{BC}=−15.8
δ	2.58	3.02	2.90	2.82
BR-XIII	J_{BX}=2.0	J_{AB}=14.0	J_{AB}=14.0	J_{AX}=2.5
	J_{CX}=4.0	J_{AC}=2.5	J_{BX}=2.0	J_{CX}=4.0
	J_{AX}=−14.0	J_{AX}=−14.0	J_{BC}=−18.8	J_{BC}=−18.5
δ	2.58	3.01	2.90	2.81
BR-III	J_{BX}=2.0	J_{AB}=14.5	J_{AB}=14.5	J_{AC}=2.5
	J_{CX}=3.5	J_{AC}=2.5	J_{BX}=−2.0	J_{CX}=3.5
	J_{AX}=−13.5	J_{AX}=−13.5	J_{BC}=−17.0	J_{BC}=−17.0

δ, ppm downfield from (CH$_3$)$_4$Si; J in Hz from 500 MHz spectra.
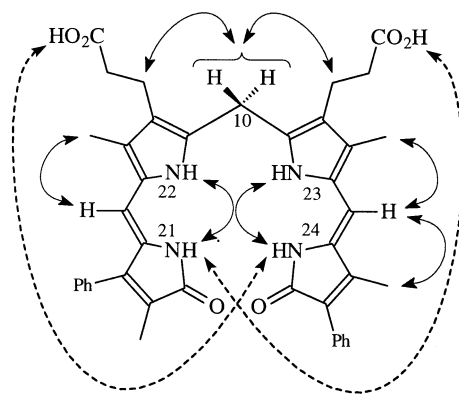

Figure 3. Selected nuclear Overhauser effects (NOEs) found in phenylrubin **1**. Weaker NOEs are noted by dashed arrows. NOEs similar to those of the left half of **1** are found in **2**, whereas NOEs similar to those of the right half of **1** are found in **3**.
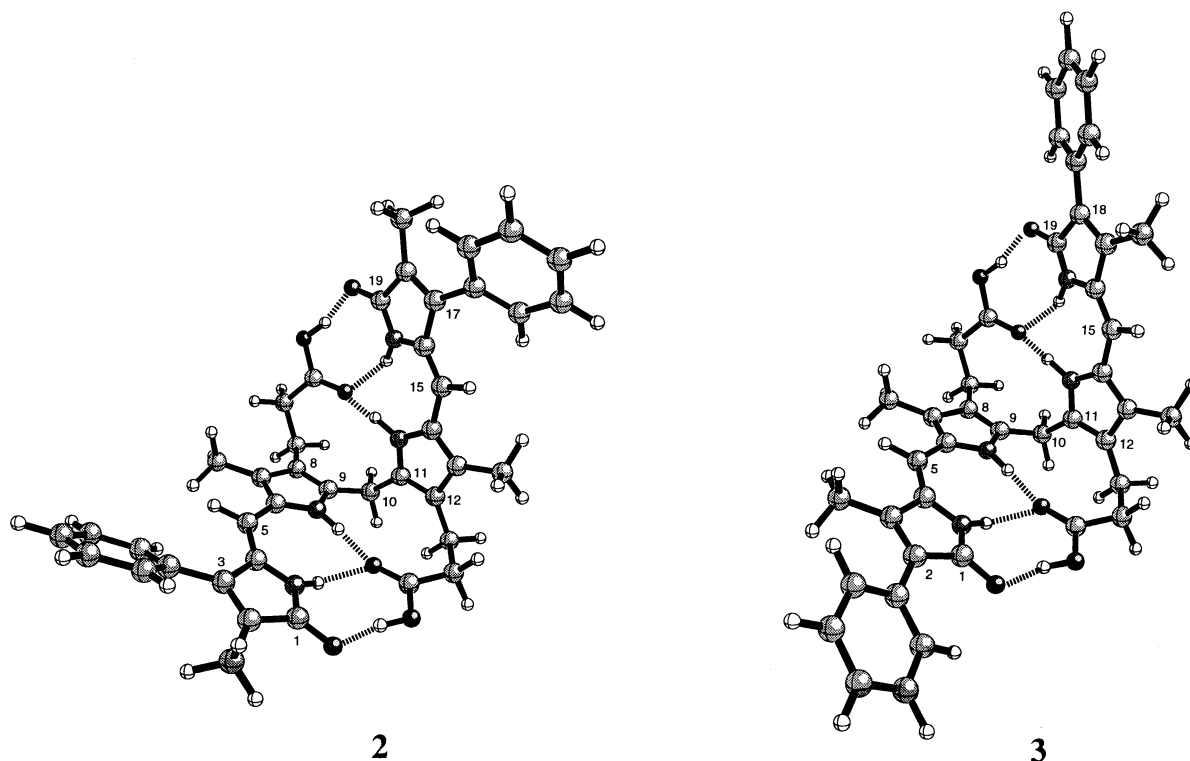
2   **3**

Figure 4. Ball and Stick drawings of **2** and **3** in their energy-minimized conformation, as determined by molecular mechanics calculations using Sybyl (Ref. 13).

Table 4. Solvent-dependence of UV–vis spectral data of phenyl rubins **1–3** and Bilirubins-IXα, XIIIα and IIIα (BR-IX, BR-XIII and BR-III)

Cpd	$\Delta\varepsilon^{max}(\lambda^{max}$, nm)					
	Benzene	CHCl$_3$	(CH$_3$)$_2$CO	CH$_3$OH	CH$_3$CN	(CH$_3$)$_2$SO
1	61,300 (452)	63,300 (451)	60,600 (446)	61,400 (445)	59,200 (443)	64,200 (447)
	50,300 (423)[a]	52,400 (423)[a]	50,300 (419)[a]	47,700 (410)[a]	48,600 (417)[a]	46,900 (409)[a]
2	56,300 (448)	55,500 (446)	52,400 (440)	55,100 (440)	53,100 (439)	60,800 (441)
	53,700 (436)[a]	53,800 (435)[a]	49,000 (424)[a]	49,400 (420)[a]	49,500 (423)[a]	53,300 (421)[a]
3	65,500 (465)	66,000 (454)	64,300 (449)	61,200 (446)	62,300 (440)	67,300 (453)
	56,000 (423)[a]	61,900 (438)[a]	60,700 (435)[a]	54,000 (426)[a]	58,500 (431)[a]	54,900 (422)[a]
BR	53,300 (455)	55,800 (453)	56,400 (449)	54,400 (449)	54,000 (447)	58,800 (455)
IX	46,700 (433)[a]	49,500 (432)[a]	49,900 (429)[a]	44,600 (417)[a]	45,000 (421)[a]	43,000 (415)[a]
BR	45,580 (447)	46,920 (450)	46,600 (447)	45,300 (446)	47,000 (445)	47,800 (446)
XIII		34,600 (415)[a]	37,500 (416)[a]	39,400 (417)[a]	37,700 (415)[a]
BR	61,700 (460)	64,600 (456)	62,400 (451)	60,700 (451)	62,400 (451)	67,800 (459)
III	48,100 (426)[a]	49,600 (424)[a]	50,900 (424)[a]	49,100 (417)[a]	51,200 (423)[a]	48,800 (416)[a]

At 22°C in concentrations ~1.4×10^{-5} M.
[a] Shoulders (or) inflections were determined by first and second derivative spectra.

Table 5. Comparison of circular dichroism and UV–visible spectroscopic data for phenyl rubins **1–3** and bilirubins-IXα, XIIIα and IIIα (BR-IX, BR-XIII and BR-III) in CHCl$_3$ solutions containing quinine

Pigment	CD			UV	
	$\Delta\varepsilon^{max}(\lambda_1)$	λ_2 at $\Delta\varepsilon(0)$	$\Delta\varepsilon^{max}(\lambda_3)$	ε^{max}	λ (nm)
1	+29 (400)	419	−52 (446)	62,300	451
2	+37 (396)	415	−62 (443)	56,700	446
3	+33 (402)	423	−55 (452)	64,100	454
BR-IX	+39 (405)	425	−64 (453)	56,800	455
BR-XIII	+27 (402)	424	−46 (454)	45,900	450
BR-III	+58 (408)	427	−89 (456)	63,300	458

Pigment conc. ~1.4×10^{-5} M; quinine conc. ~4.2×10^{-3} M; pigment: quinine molar ratio=~1:300.

The IX isomers have λ^{max} lying between those of XIII and III, and the ε values are noticeably larger for the phenyl analogs of bilirubins-IIIα, IXα and XIIIα. Whether phenyl or vinyl, however, the long wavelength absorption is characteristically broadened or dimpled due to exciton coupling between the two component dipyrrinone chromophores of each rubin. Such exciton coupling may be seen even more clearly by circular dichroism spectroscopy.

2.4. Circular dichroism spectra

Earlier studies have shown that bilirubin-IXα and related rubins exhibit an induced circular dichroism (CD) in CHCl$_3$ solvent in the presence of quinine and other optically active
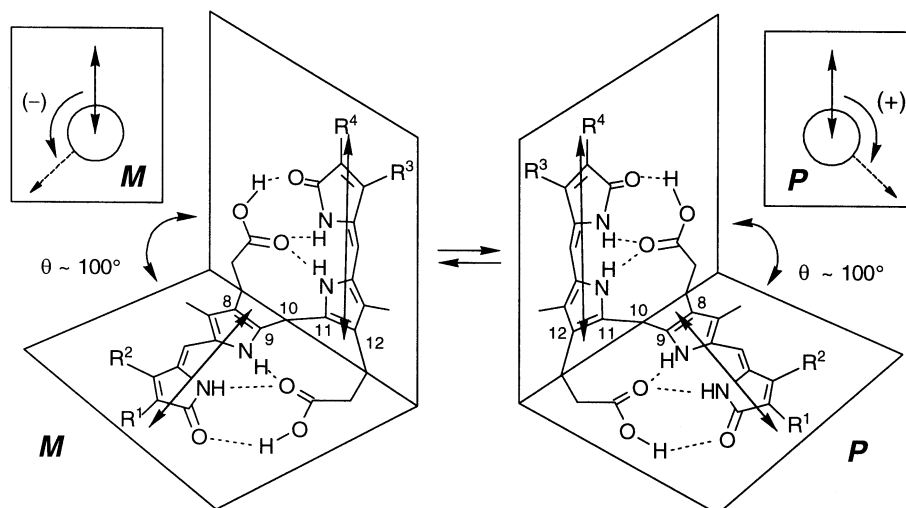
Figure 5. Interconverting intramolecularly hydrogen-bonded enantiomeric conformers of mesobilirubins **1–4** and bilirubin (see Fig. 1). The double headed arrows represent the dipyrrinone long-wavelength electric transition moments (dipoles). The relative helicities (**M**, minus, or **P**, plus) of the vectors are shown (inset) for each enantiomer. Hydrogen bonds are shown by dashed lines.

amines.[14,15] Phenylrubins **1–3** are no exception and exhibit strong bisignate CD Cotton effects (Table 5) associated with the two exciton transitions at long wavelengths (that were overlapping and less distinct in the UV–vis spectra). The two-dipyrrinone chromophores of each rubin have strongly allowed long wavelength electronic transitions (Table 4), making them excellent candidates for transition dipole–dipole interaction (exciton coupling). Such intramolecular exciton interaction or resonance splitting produces two long wavelength transitions in the UV–vis spectrum and two corresponding, but oppositely signed, bands in the CD spectrum.[14,16] According to exciton chirality theory, a long-wavelength negative and short-wavelength positive CD couplet exhibits negative exciton chirality and corresponds to a negative helical disposition of the relevant dipyrrinone long-wavelength transition dipoles. Usually this corresponds to the *M*-helical enantiomeric type of Fig. 5. But, as has been shown previously, opening of the interplanar angle of either enantiomer without inverting molecular helicity also can cause the transition moments to invert helicity and invert the Cotton effect signs of the CD couplet.[17]

In a nonpolar, aprotic solvent such as chloroform, the conformational equilibrium between bilirubin enantiomers (Fig. 5) can be displaced from 1:1 by adding a chiral recognition agent such as quinine or other optically active amines.[14,15] This leads typically to an intense bisignate induced CD Cotton effect, as has been noted previously for bilirubin in aqueous buffers with added albumin. The strong, negative exciton chirality CDs observed in the presence of quinine (Table 5) is characteristic of an exciton system in which the two dipyrrinone chromophores of the bichromophoric rubin molecule interact by coupling locally excited π–π^* transitions (electric dipole transition moment coupling). Interestingly, at the same molar ratio of alkaloid/pigment of $\sim$300:1,[14] which typically gives optimal Cotton effects, the intensities are rather similar—except for bilirubin-IIIα, which shows nearly double the intensity of the others.

When human serum albumin (HSA) is used as the chiral complexation agent in aqueous (pH 7.4 Tris buffer) solutions,[18] all but **2** exhibit moderately intense positive chirality bisignate Cotton effects (Fig. 6A). Phenylrubin **2** exhibits a negative-exciton chirality, and its counterpart, bilirubin-XIIIα, exhibits the weakest of the five positive exciton chirality Cotton effects, suggesting weaker or even reversed enantioselectivity by the protein. Interestingly, both **3** and bilirubin-IIIα give the most intense Cotton effects, suggesting that the *exo* substituent is important for favorable binding to the chiral complexation agent.

Adding trace amounts of CHCl$_3$ (μL/mL) to buffered aqueous HSA solutions of the rubins (except for **2**) leads to inverted Cotton effect signs (Fig. 6B, Table 6), as noted previously.[17] Upon addition of 5 μL CHCl$_3$, all but bilirubin-IXα and IIIα show a negative exciton chirality. The Cotton effects of **1** and **2** become especially intense. Addition of a second 5 μL aliquot of CHCl$_3$ causes all rubins to exhibit a negative exciton chirality and leads to increased magnitudes. The Cotton effect magnitudes of **1** and **2** remain exceptionally strong relative to the other rubins. At a total of 15 μL/5 mL, further Cotton effect intensification is seen for bilirubins IIIα, IXα and XIIIα, while that of **1** is changed little, and solutions of **2** and **3** have exceeded the saturation limit. The initially large Cotton effects of the symmetric *exo*-phenyl (**3**) and *exo*-vinyl rubins on HSA and their sluggishness to invert with added CHCl$_3$ suggest that they are tightly bound to HSA in a favorable binding site. Apparently it is the location (*exo*) of the aryl and vinyl groups rather than their presence that is responsible for the phenomenon.

2.5. Polarity and solubility

Fig. 7 shows HPLC chromatograms of mixtures of bilirubins IIIα, IXα and XIIIα and diphenylrubins **1–3**. Their relative retention factors are bilirubin-XIIIα, 1.00; bilirubin-IXα, 1.13; bilirubin IIIα and **2**, 1.28; **1**, 1.51 and **3**, 1.76, indicating that **1–3** are somewhat more lipophilic than their
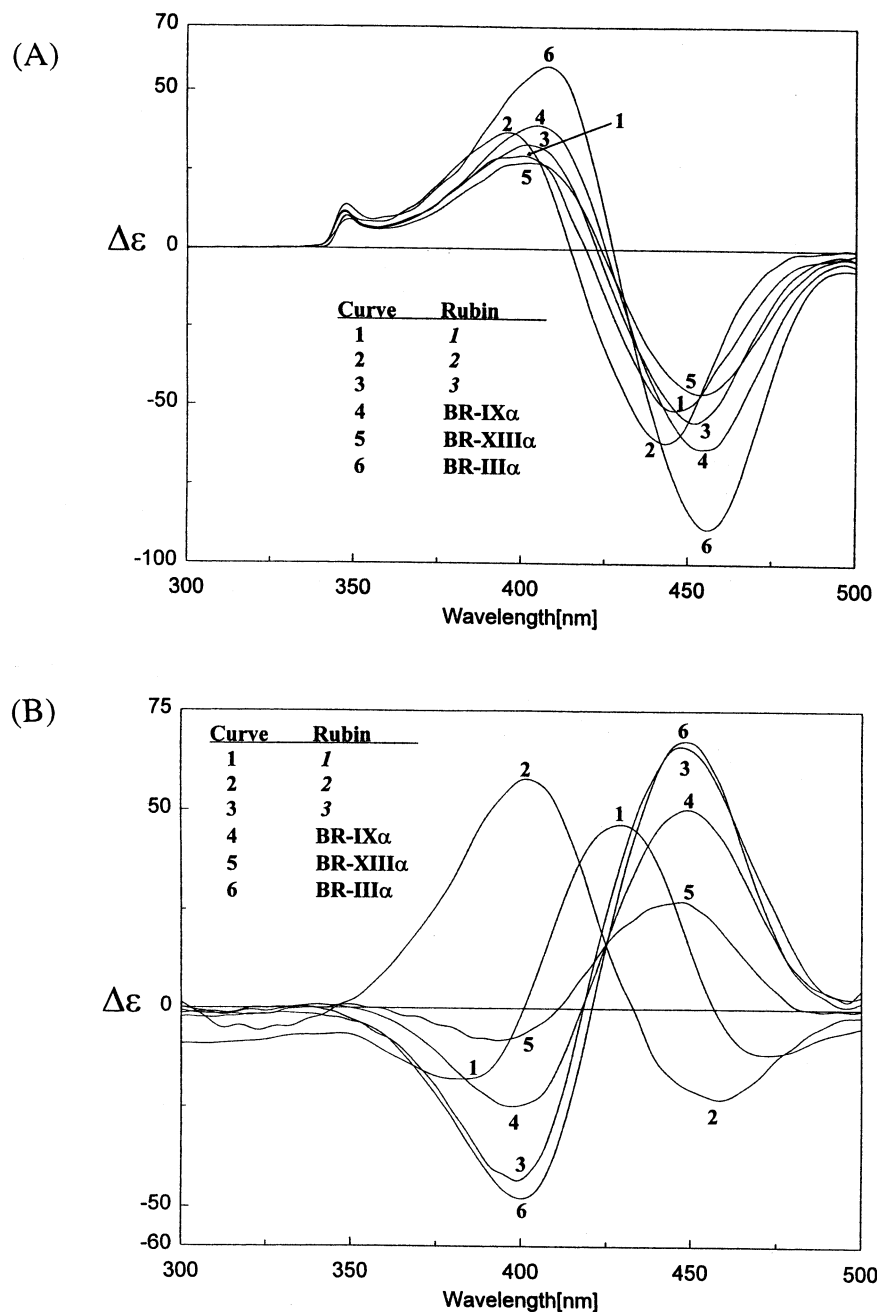
Figure 6. Circular dichroism spectra of 1.4×10^{-5} M **1–3** and their bilirubin parents in CHCl$_3$ in the presence of (A) ca. 4.2×10^{-3} M quinine and (B) ca. 2.8×10^{-5} M HSA in pH 7.4 Tris buffer at 22°C. The compound numbers are indicated on each CD curve.

vinyl counterparts. Bilirubin IIIα and diphenylrubin **2**, the phenyl counterpart of bilirubin-XIIIα, had identical retention times and were unresolved when chromatographed together. Similarly, on silica TLC, **1–3** have an $R_f\sim0.58$, whereas the vinyl analogs have R_f 0.53 (solvent 99:1 CH$_2$Cl$_2$/MeOH by vol). For bilirubins with natural side-chains, lipophilicity increases in the order XIIIα, IXα, IIIα, and the same relative order is maintained for the corresponding phenyl substituted compounds **1–3**. Taken collectively, the polarity and solubility characteristics of **1–3** are consistent with the propionic acid side-chains being involved in intramolecular hydrogen bonding and unavailable for solvent interaction.

2.6. Hepatic metabolism

Bilirubin is cleared from the circulation in healthy humans, rats and other mammals by the liver, where it undergoes enzymic conversion to two isomeric monoglucuronides. These are partly converted by the same enzyme to bilirubin diglucuronide. The resulting mixture of three acyl glucuronides is secreted from the liver into bile. Formation of the glucuronides is catalyzed by a specific isoform, UGT1A1, of the uridine diphosphoglucuronosyl transferase family.[1–3] This particular isoform is not expressed in homozygotes of the mutant strain of rats known as Gunn rats. In these animals, bilirubin glucuronides are not formed and are not

Table 6. Influence of chloroform on the circular dichroism spectra for phenyl-rubins **1**–**3** and bilirubins-IXα, XIIIα and IIIα (BR-IX, BR-XIII and BR-III) in pH 7.4 Tris buffer containing HSA

Pigment	CHCl$_3$ (µL)	CD			UV	
		$\Delta\varepsilon^{max}(\lambda_1)$	λ_2 at $\Delta\varepsilon(0)$	$\Delta\varepsilon^{max}(\lambda_3)$	ε^{max}	λ (nm)
1	0	−18 (382)	401	+47 (429)	52,660	441
2		+58 (402)	433	−23 (458)	54,300	451
3		−43 (399)	418	+66 (447)	57,300	449
BR-IX		−25 (398)	418	+50 (449)	46,070	459
BR-XIII		−8 (393)	411	+27 (447)	37,670	455
BR-III		−63 (408)	421	+67 (449)	54,470	462
1	5	+108 (400)	419	−179 (449)	65,980	451
2		+145 (399)	417	−225 (446)	62,100	450
3		+14 (403)	423	−21 (453)	34,300	449
BR-IX		−9 (395)	412	+25 (455)	46,050	458
BR-XIII		+12 (404)	431	−15 (460)	39,570	451
BR-III		−17 (397)	418	+23 (443)	55,570	461
1	10	+129 (399)	418	−214 (448)	65,460	451
2		+150 (398)	417	−239 (446)	62,600	450
3		+15 (402)	422	−22 (452)	25,300	452
BR-IX		+20 (404)	427	−32 (456)	49,850	458
BR-XIII		+39 (399)	422	−69 (452)	40,930	449
BR-III		+21 (406)	425	−42 (455)	56,620	460
1	15	+134 (399)	418	−223 (448)	66,330	451
2		a	a	a	a	a
3		a	a	a	a	a
BR-IX		+43 (403)	424	−71 (455)	52,550	456
BR-XIII		+51 (400)	421	−94 (452)	43,830	449
BR-III		+40 (406)	425	−72 (454)	58,130	460

Chloroform was added to 5 mL solutions that were ~1.4×10^{-5} M in pigment and 1:2 molar ratio of pigment to HSA (human serum albumin) at 22°C.
[a] Solubility limit of CHCl$_3$ exceeded.

present in bile, and unconjugated bilirubin accumulates in their circulation and extravascular tissues.

When compounds **1**–**3** were injected intravenously as 0.25 mg bolus doses into homozygous Gunn rats they were not excreted in bile, either as the intact pigments or as metabolites. In contrast, in normal rats each of the three was excreted in bile as a pair of metabolites after intravenous administration (Fig. 8). Since these metabolites were observed only in normal rats and not in Gunn rats, it is logical to assume that they are acyl glucuronides forme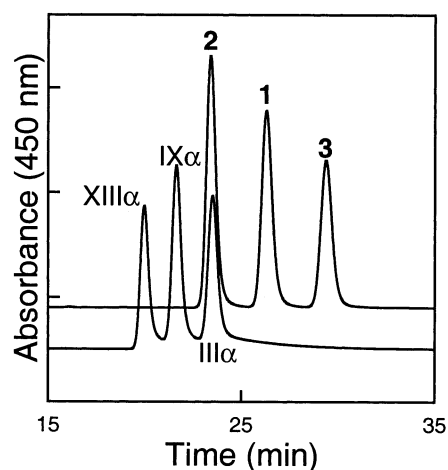d by UGT1A1 catalysis, with the most polar metabolite from each compound being the diglucuronide and the least polar, the monoglucuronide. The absorption spectra of the metabolites (Fig. 9, Table 7) are consistent with that assumption. In each case, glucuronidation led to the appearance of a weak shoulder on the short wavelength side of the main absorption band, which is more pronounced for the diglucuronide than the monoglucuronide. Acyl glucuronides of bilirubin, mesobilirubin and other bilirubins show the same phenomenon. For compound **2**, identification of its metabolites as acyl glucuronides was confirmed by their hydrolysis to the parent pigment with both β-glucuronidase and dilute NaOH (Fig. 10). Only one monoglucuronide HPLC peak was detected for the unsymmetrically substituted biphenyl compound **1**, rather than the two diastereomer peaks expected. Whether this reflects poor HPLC resolution or regiospecific glucuronidation is unclear. The peak was, however, very slightly less symmetrical than the peaks of the monoglucuronides of the symmetrical isomers **2** and **3**, suggesting that two similar components might have been present.

These metabolic studies show that biphenyl compounds **1**–**3** are metabolized much like bilirubin, being converted to more polar cholephilic mono and diglucuronides by UGT1A1. Their rates of excretion into bile as glucuronides were slower than for similar compounds without phenyl substitution, as shown by the rather broad, tailing biliary excretion curves (Fig. 8). This could be a consequence of slower uptake, impaired glucuronidation or retarded efflux from the liver into bile. Our data is insufficient to distinguish these possibilities. The data do show, however, that the ratio of mono to diconjugates formed from each compound is highly dependent on the positions of the phenyl groups. The proportion of diglucuronide was highest for the least
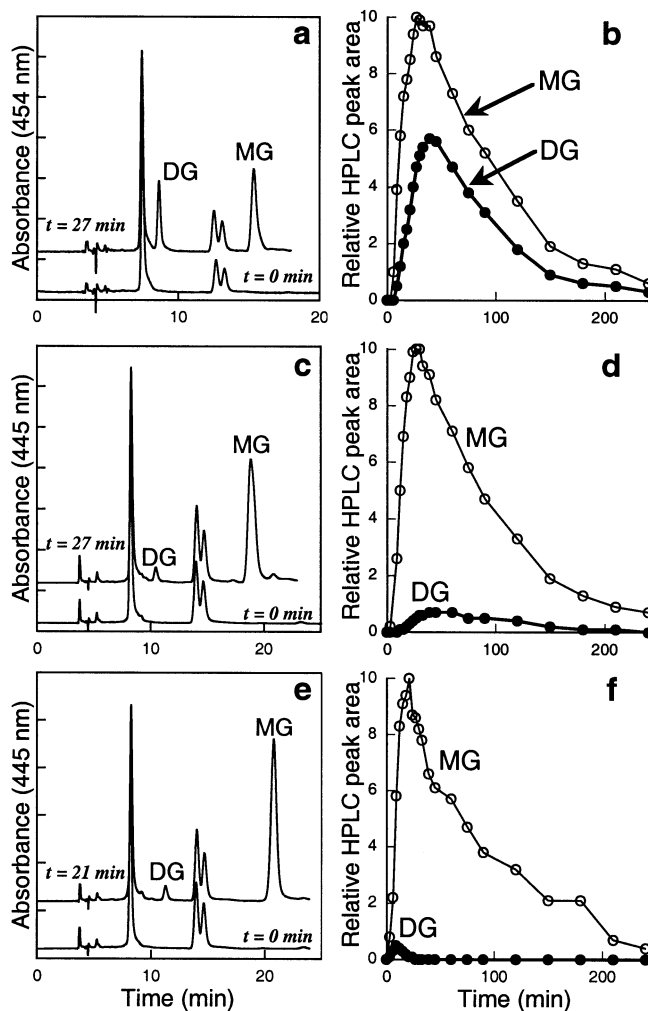

Figure 7. Superimposed reverse phase HPLC chromatograms of mixtures containing (lower) bilirubin XIIIα, IXα and IIIα and (upper) diphenyl bilirubins XIIIα (**2**), IXα (**1**) and IIIα (**3**). The mobile phase was 0.1 M di-*n*-octylamine acetate in 5% water/MeOH at a flow-rate of 0.75 mL/min.

Figure 8. Metabolism of diphenyl bilirubins XIIIα (**2**), IXα (**1**) and IIIα (**3**) in the rat. Panels **a**, **c** and **d** show HPLC chromatograms of bile before (*t*=0) and after (*t*=21 or 27 min) injecting 0.25 mg of **2**, **1** and **3**, respectively, intravenously into adult male Sprague-Dawley rats. The *t*=0 chromatograms show the presence of bilirubin diglucuronide (near 8 min) and its two diastereomeric monoglucuronides (near 14 min). MG and DG indicate, respectively, the mono and diglucuronide of the injected pigment. Panels **b**, **d** and **f** show biliary excretion curves for the mono and glucuronides of **2**, **1** and **3**, respectively, derived from the peak areas of the corresponding peaks in HPLC chromatograms of bile.
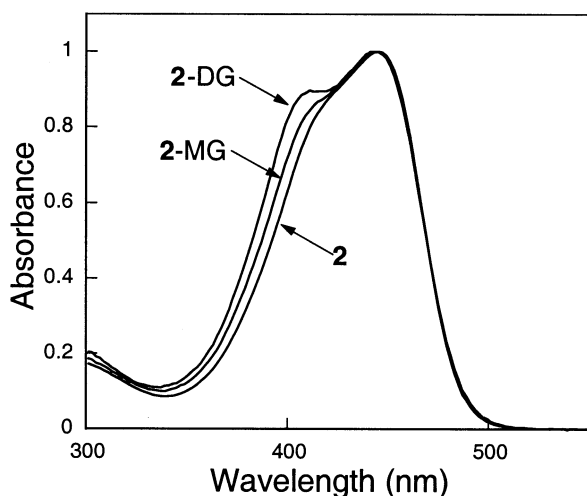

Figure 9. Normalized absorbance spectra of diphenyl bilirubin XIIIα (**2**) and its mono and diglucuronides obtained by diode array scanning of the corresponding HPLC chromatogram peaks.

lipophilic isomer **2**, in which the two phenyl groups are at the *endo* positions of the lactam rings, and lowest for the isomer **3** with phenyl groups at the two *exo* positions. The unsymmetrical isomer **1**, with one *endo* and one *exo* phenyl group, yielded an intermediate proportion of diglucuronide. We observed the same relationship between lipophilicity and the proportion of diglucuronide previously for lipophilic rubins substituted with *n*-butyl groups. However, we have also observed exclusive monoglucuronide

Table 7. Absorption spectra of diphenyl bilirubins **1–3** and their mono- (MG) and di- (DG) glucuronides. Obtained from diode array spectra of HPLC eluates in 0.1 M di-*n*-octylamine acetate in MeOH containing 8% water (sh indicates shoulder)

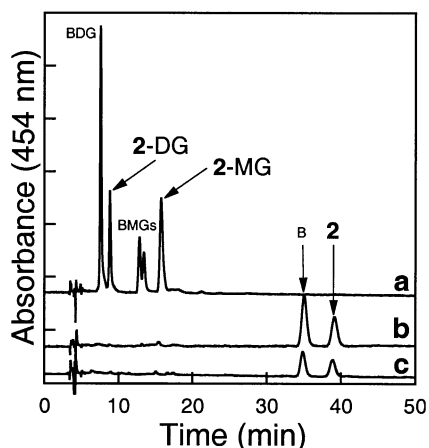| Pigment	λ (nm)		
	Parent	MG	DG
1 (IXα)	450, 420 (sh)	448, 418 (sh)	448, 412 (sh)
2 (XIIIα)	444, 416 (sh)	444, 410 (sh)	444, 408
3 (IIIα)	454, 422 (sh)	452, 418 (sh)	454, 414 (sh)

Figure 10. Hydrolysis of bile from a rat injected with diphenyl bilirubin XIIIα (**2**). HPLC chromatogram **a** is of bile collected 39 min after injection of pigment. Chromatogram **b** is of bile collected 45 min after injection and treated with aqueous β-glucuronidase. Chromatogram **c** is of bile collected 24 min after injection and treated with dilute aqueous NaOH. B, BMGs and BDG indicate bilirubin and its mono and diglucuronides, respectively. DG and MG indicate mono and diglucuronide, respectively.

formation for bilirubins substituted with two methyl groups at C10, which are much less lipophilic than bilirubin.[19] Not knowing the extinction coefficients for the glucuronides, we were unable to calculate the exact ratio of mono to diglucuronidation for each compound. However, since the aglycones and their glucuronides have very similar absorption spectra (Fig. 10), it is likely that mono to diglucuronide ratios computed from the corresponding peak areas are close to the true values.

These studies show that bilirubins containing bulky phenyl groups at the *endo* or *exo* positions have similar three-dimensional structures to natural bilirubin, but are more lipophilic. In the rat, they are metabolized, like bilirubin, to mono and diglucuronides that are excreted in bile. However, the proportion of diglucuronide formation is much less than for bilirubin and the overall rate of excretion of the glucuronides into bile is slower than for bilirubin glucuronides with simple alkyl groups (Me, Et or vinyl) in place of the phenyl groups. Despite having relatively bulky phenyl groups on the lactam rings, compounds **1–3** are substrates of UGT1A1 in vivo.

3. Experimental

All ultraviolet–visible (UV–vis) spectra were recorded on a Perkin–Elmer λ-12 spectrophotometer, and all circular dichroism (CD) spectra were recorded on a Jasco J-600 instrument. Nuclear magnetic resonance (NMR) spectra were obtained on GE QE-300 spectrometer operating at 300 MHz, or on a Varian Unity Plus 500 MHz spectrometer in $CDCl_3$ solvent (unless otherwise specified). Chemical shifts were reported in δ ppm referenced to the residual $CHCl_3$ [1]H signal at 7.26 ppm and ^{13}C signal at 77.23 ppm. A J-modulated spin-echo experiment (Attached Proton Test) was used to assign ^{13}C NMR spectra. Melting points were taken on a MelTemp capillary apparatus and are uncorrected. Combustion analyses were carried out by Desert Analytics, Tucson, AZ. Analytical thin layer chroma-

tography was carried out on J.T. Baker silica gel IB-F plates (125 μ layers). HPLC analyses were carried out on a Perkin–Elmer Series 4 high performance liquid chromatograph with an LC-95 UV–visible spectrophotometric detector (set at 410 nm) equipped with a Beckman-Altex ultrasphere-IP 5 μm C-18 ODS column (25×0.46 cm) and a Beckman ODS precolumn (4.5×0.46 cm). For HPLC analyses of metabolites in bile, detection (HP 1100 or 1050 DAD) was in the range of ~454 nm, and the column was a Beckman-Altex ultrasphere-IP 5 μm C-18 ODS column (25×0.46 cm) fitted with a similarly packed pre-column (4.5×0.46 cm). The flow rate was 0.75 mL/min, the elution solvent was 0.1 M di-*n*-octylamine acetate in 8% aqueous methanol, and the column temperature ~34°C. Di-*n*-octylamine was obtained from Aldrich; HPLC grade MeOH from Fisher; β-glucuronidase (*E. coli* Type VII-A, 1000 units/vial), phosphatidyl choline (Type XV-E), cholesterol, taurine, sodium cholate and human serum albumin (defatted) from Sigma. All other solvents and reagents, unless otherwise specified, were purchased from Acros, Aldrich or Fisher and used as received. Spectral data were obtained in spectral grade solvents (Aldrich or Fisher).

The Ball and Stick drawings were created from the atomic coordinates of the molecular dynamics structures using the Müller and Falk 'Ball and Stick' program (Cherwell Scientific, Oxford, UK) for Macintosh. The molecular dynamics calculations were carried out on a Silicon Graphics workstation using Sybyl 6.6 with Gasteiger–Hückel calculations of electrostatic charge.

Jaundiced homozygous male Gunn rats, weighing 300–400 g, were obtained from our own colony and normal Sprague-Dawley male rats, weight ~300 g, were obtained from local commercial vendors. In vivo studies were done in a windowless room under safe lights, as described elsewhere.[19,22] Each compound was studied in a single Gunn rat and in at least two normal rats. Qualitatively similar biliary excretion curves to those depicted in Fig. 8 were obtained in replicate experiments.

3.1. CD and UV measurements

A stock solution of rubin (~$7.0×10^{-4}$ M) was prepared by dissolving an appropriate amount of the desired rubin compound in 2 mL of DMSO. Next, 100 μL of the stock solution was diluted to 5 mL (volumetric flask) with an HSA solution ~$2.8×10^{-5}$ M in pH 7.4 Tris buffer. The final concentration of the solution was ~$1.4×10^{-5}$ M in pigment. Up to four 5 mL solutions of each pigment were prepared, as needed, in 5 mL volumetric flasks. To each flask was added the indicated volume (μL) of $CHCl_3$. Gentle shaking was occasionally required to dissolve all of the $CHCl_3$ in the aqueous solution, at which point CD and UV–vis measurements were recorded.

3.1.1. 4-Methyl-3-phenyl-2-*p*-toluenesulfonyl-1*H*-pyrrole (10). *p*-Toluenesulfonylmethyl isocyanide (TosMIC)[10] (6.08 g, 31.2 mmol) and 1,1,3,3-tetramethyl guanidine (7.60 g, 65.5 mmol) were dissolved in 36 mL of a 1:1 mixture of THF–2-propanol and stirred magnetically at room temperature. A solution of 1-phenyl-2-nitro-1-propanol

acetate[11] (**15**) (6.95 g, 31.2 mmol) was added dropwise, and the mixture was stirred at room temperature overnight. It was then diluted with 70 mL of CH_2Cl_2, washed with water (2×70 mL) and brine (70 mL), and dried over anhydr. $MgSO_4$. The solvent was removed (rotary evaporator), and the residue was crystallized from CH_2Cl_2–hexane to yield 5.14 g (53%) of a tan solid. An analytical sample was prepared by recrystallization from CH_2Cl_2–hexane. Colorless crystals of **10** were collected and dried over P_2O_5 in a drying pistol overnight. Mp 202–203°C; IR (KBr) ν: 3380, 1596, 1313, 1301, 1211, 1143, 1081, 705, 589 cm^{-1}; ^1H NMR δ: 9.03 (1H, brs), 7.38–7.06 (5H, m), 6.79 (1H, d, J=2 Hz), 2.32 (3H, s), 1.92 (3H, s) ppm; ^{13}C NMR δ: 143.66, 139.53, 132.84, 130.75, 129.79, 129.44, 127.97, 127.56, 127.14, 125.01, 121.48, 120.22, 21.64, 10.53 ppm; MS: m/z (relative intensity) 379(12), 311(100), 231(30), 172(40), 117(20), 91(10) amu. Anal. calcd for $C_{18}H_{17}NO_2S$ (311.4): C, 69.43; H, 5.50; N, 4.40%. Anal. calcd for $C_{18}H_{17}NO_2S\cdot1/4H_2O$ (315.9): C, 68.44; H, 5.58; N, 4.43%. Found: C, 68.42; H, 5.56; N, 4.68%.

3.1.2. 5-Bromo-4-methyl-3-phenyl-2-*p*-toluenesulfonyl-1*H*-pyrrole (12).

4-Methyl-3-phenyl-2-*p*-toluenesulfonyl-1*H*-pyrrole (**10**) (2.00 g, 6.43 mmol) was dissolved in 50 mL of CH_2Cl_2 and stirred in an ice bath magnetically. A solution of phenyltrimethyl ammonium tribromide (PTT) (5.07 g, 13.5 mmol) in 100 mL of CH_2Cl_2 was added dropwise and the resulting yellow-orange solution was stirred at 0°C for 30 min. It was then washed with aq. sodium bisulfite (3×150 mL) and brine (150 mL), then dried over anhydr. $MgSO_4$. The solvent was removed using a rotary evaporator to yield a colorless solid (2.36 g, 94%). An analytical sample was prepared by the addition of hexane to a CH_2Cl_2 solution of the pyrrole. Colorless crystals of **12** were collected and dried over P_2O_5 in a drying pistol overnight. Mp 172–174°C; IR (KBr) ν: 3270, 1445, 1317, 1142, 1192, 1085, 772, 707, 590 cm^{-1}; ^1H NMR δ: 9.12 (1H, brs), 7.37–7.08 (5H, m), 2.33 (3H, s), 1.85 (3H, s) ppm; ^{13}C NMR δ: 144.00, 139.14, 132.25, 130.65, 130.54, 129.76, 129.54, 128.11, 128.05, 127.32, 121.43, 104.45, 21.67, 10.50 ppm; MS: m/z (relative intensity) 391(100), 325(10), 245(32), 154(70), 127(22), 91(15) amu. Anal calcd for $C_{18}H_{16}BrNO_2S$ (390.3): C, 55.39; H, 4.13; N, 3.59. Found: C, 55.10; H, 3.96; N; 3.58.

3.1.3. 3-Methyl-4-phenyl-5-*p*-toluenesulfonyl-3-pyrrolin-2-one (8).

5-Bromo-4-methyl-3-phenyl-2-*p*-toluenesul-fonyl-1*H*-pyrrole (**12**) (2.00 g, 5.13 mmol) was dissolved in 40 mL of TFA and 8 mL of water, then stirred at room temperature overnight. The resulting dark solution was diluted with 100 mL of CH_2Cl_2 and washed sequentially with water (2×100 mL), aq. sodium bicarbonate (2× 100 mL) and brine (100 mL); then it was dried over anhydr. $MgSO_4$. The solvent was removed on a rotary evaporator to yield 1.63 g (98%) of a light gray powder. Colorless crystals were obtained by the addition of hexane to a CH_2Cl_2 solution of pyrrolinone **8**. They were collected and dried over P_2O_5 in a drying pistol overnight. Mp 80–82°C; IR (KBr) ν: 3431, 1700, 1446, 1357, 1136, 1083, 816, 636, 547 cm^{-1}; ^1H NMR δ: 7.46–7.23 (5H, m), 7.40 (2H, d, J=8 Hz), 7.22 (2H, d, J=8 Hz), 6.85 (1H, s), 5.70 (1H, s), 2.42 (3H, s), 1.80 (3H, s) ppm; ^{13}C NMR δ: 173.17, 146.84, 145.89, 144.77, 134.06, 131.33, 129.84, 129.70, 129.58,

129.05, 128.63, 77.72, 21.80, 10.13 ppm. Anal. calcd for $C_{18}H_{17}NO_3S$ (327.4): C, 66.03; H, 5.24; N, 4.28. Found: C, 65.76; H, 5.45; N, 4.60.

3.1.4. 3-Methyl-4-phenyl-3-pyrrolin-2-one (6).

3-Methyl-4-phenyl-5-*p*-toluenesulfonyl-3-pyrrolin-2-one (**8**) (1.63 g, 5.01 mmol) and sodium borohydride (0.23 g, 6.01 mmol) were stirred in 65 mL of absolute ethanol at room temperature for 10 min. The solution was then diluted with 65 mL of CH_2Cl_2, washed with water (2×65 mL) and brine (65 mL), and dried over anhydr. $MgSO_4$. The solvent was removed (rotary evaporator), and the residue was crystallized from CH_2Cl_2–hexane to afford a light tan powder (0.76 g, 88%). An analytical sample was prepared by precipitation of a CH_2Cl_2 solution with hexane. Colorless crystals of **6** were collected and dried over P_2O_5 in a drying pistol overnight. Mp 155–158°C [lit.[20] mp 155–158°C]; IR (KBr) ν: 3432, 1687, 1499, 1452, 1364, 766, 693, 614 cm^{-1}; ^1H NMR δ: 7.50–7.30 (5H, m), 7.05 (1H, brs), 4.23 (2H, d, J=1 Hz), 2.10 (3H, s) ppm; ^{13}C NMR δ: 174.92, 151.21, 132.53, 131.83, 129.31, 128.44, 127.85, 50.46, 14.48 ppm.

3.1.5. 5,5′-Diformyl-4,4′-dimethyl-5,5′-bis(2-carboxy-ethyl)-2,2′-dipyrrylmethane (14).

Dipyrrylmethane dimethyl ester **13**[7,9,10] (0.30 g, 0.75 mmol) was dissolved in 30 mL of methanol and 10 mL of 6 M aq. KOH. The solution was heated at reflux for 2 h, then cooled in an ice bath, diluted with water, and acidified with acetic acid to form a tan precipitate. The solids were collected by vacuum filtration and air dried to afford diacid **14** (0.25 g, 90%), which was used directly in the next step. Mp 248–250°C; IR (KBr) ν: 3248, 2919, 1713, 1619, 1449, 1384, 1207, 873 cm^{-1}; ^1H NMR (DMSO-d$_6$) δ: 12.00 (2H, s), 11.48 (2H, s), 9.48 (2H, s), 3.91 (2H, s), 2.51 (4H, t, J=8 Hz), 2.18 (6H, s), 2.06 (4H, t, J=8 Hz) ppm; ^{13}C NMR (DMSO-d$_6$) δ: 176.71, 173.75, 134.57, 130.41, 128.01, 120.73, 34.21, 22.46, 18.63, 8.46 ppm.

3.1.6. 3,17-Des-vinyl-3,17-bis-phenyl-bilirubin-XIIIα (2).

In a 50 mL round bottomed flask 3-methyl-4-phenyl-3-pyrrolin-2-one (**6**) (0.253 g, 1.46 mmol) and diformyl-dipyrrylmethane **14** (0.129 g, 0.341 mmol) were dissolved in 55 mL of 2-propanol and 0.28 mL of piperidine. The solution was heated at reflux overnight, during which time the product precipitated. The mixture was chilled in an ice bath, and the solids were collected by vacuum filtration then washed with water (2×10 mL). The yellow-orange solid was air dried to afford pure **2** (0.081 g, 37%). Mp 320–322°C; IR (KBr) ν: 3417, 2920, 1692, 1634, 1443, 1385, 1252, 1020, 700 cm^{-1}; ^1H NMR δ: 13.69 (2H, brs), 10.90 (2H, s), 9.28 (2H, s), 7.48–7.28 (10H, m), 5.97 (2H, s), 4.08 (2H, s), 3.01 (2H, ddd, J=15.0, 3.0, −14.5 Hz), 2.89 (2H, ddd, J=13.0, −19.5, 1.5 Hz), 2.79 (2H, ddd, J=3.0, −19.5, 4.0 Hz), 2.56 (2H, ddd, J=−14.5, 1.5, 4.0 Hz), 2.03 (6H, s), 1.91 (6H, s) ppm; ^{13}C NMR δ: 179.85, 174.26, 146.45, 133.86, 132.32, 129.75, 128.82, 128.69, 128.66, 124.97, 124.79, 124.53, 119.86, 104.56, 32.79, 22.49, 18.79, 10.32, 9.06 ppm. Anal. calcd for $C_{41}H_{40}N_4O_6$ (684.8): C, 71.91; H, 5.89; N, 8.18. Found: C, 71.95; H, 6.05; N, 8.08.

3.1.7. 3-Methyl-4-phenyl-2-*p*-toluenesulfonyl-1*H*-pyrrole (11).

4-Methyl-3-phenyl-2-*p*-toluene-sulfonyl-1*H*-pyrrole (**10**) (6.00 g, 19.3 mmol) was dissolved in 19.2 mL of

TFA and 172.8 mL of CH_2Cl_2 to make a 0.1 M solution. The solution was stirred at room temperature for 4 days, during which time it darkened. It was washed with water (2× 200 mL), aq. sodium bicarbonate (2×200 mL) and brine (200 mL), then dried over anhydr. $MgSO_4$. The solvent was removed on a rotary evaporator, and the residue was crystallized from ethyl acetate–hexane to afford 3.92 g (65%) of a tan solid. Colorless crystals of **11** were obtained by precipitation from ethyl acetate–hexane. They were collected and dried over P_2O_5 in a drying pistol overnight. Mp 117–118°C; IR (KBr) ν: 3400, 1664, 1442, 1302, 1141, 1087, 706, 691, 599 cm^{-1}; ^{1}H NMR δ: 9.33 (1H, brs), 7.82 (2H, d, J=8 Hz), 7.36–7.28 (5H, m), 7.29 (2H, d, J=8 Hz), 7.00 (1H, d, J=3 Hz), 2.41 (3H, s), 2.30 (3H, s) ppm; ^{13}C NMR δ: 143.95, 139.97, 134.63, 130.02, 128.65, 128.53, 127.95, 126.95, 126.74, 125.02, 123.42, 120.93, 21.69, 10.40 ppm; MS: *m/z* (relative intensity) 311(100), 246(12), 172(10), 154(12), 128(10) amu. Anal. calcd for $C_{18}H_{17}NO_2S$ (311.4): C, 69.43; H, 5.50; N, 4.40. Anal. calcd for $C_{18}H_{17}NO_2S \cdot 1/4H_2O$ (315.9): C, 68.44; H, 5.58; N, 4.43. Found: C, 68.00; H, 5.33; N, 4.58.

3.1.8. 4-Methyl-3-phenyl-5-*p*-toluenesulfonyl-3-pyrrolin-2-one (9).

3-Methyl-4-phenyl-2-*p*-toluenesulfonyl-1*H*-pyrrole (**11**) (1.00 g, 3.21 mmol) was dissolved in acetic acid (40 mL) and 30% aq. hydrogen peroxide (0.55 mL, 4.8 mmol) and stirred at room temperature for 3 days. The solution was diluted with CH_2Cl_2 (100 mL), washed with water (2×100 mL) and brine (100 mL), and dried over anhyd. $MgSO_4$. Removal of the solvent by rotary evaporation gave a crude solid that was purified by radial chromatography (2% methanol in CH_2Cl_2 eluent) to yield 0.28 g (25%) of pure product. Mp 133–134°C; IR (KBr) ν: 3425, 1702, 1386, 1317, 1136, 1081, 700, 587 cm^{-1}; ^{1}H NMR δ: 7.73 (2H, d, J=8 Hz), 7.34–7.28 (5H, m), 7.15 (1H, s), 7.06 (2H, d, J=8 Hz), 5.17 (1H, s), 2.34 (3H, s), 2.32 (3H, s) ppm; ^{13}C NMR δ: 172.02, 146.29, 144.69, 136.68, 130.70, 129.96, 129.63, 129.52, 129.03, 128.76, 128.47, 79.45, 21.77, 14.51 ppm. Anal. calcd for $C_{18}H_{17}NO_3S$ (327.4): C, 66.03; H, 5.24; N, 4.28. Found: C, 65.71; H, 5.05; N, 4.30.

3.1.9. 4-Methyl-3-phenyl-3-pyrrolin-2-one (7).

4-Methyl-3-phenyl-5-*p*-toluenesulfonyl-3-pyrrolin-2-one (**9**) (0.63 g, 1.93 mmol) and sodium borohydride (0.09 g, 2.32 mmol) were stirred in 25 mL of absolute ethanol at room temperature for 10 min. The solution was then diluted with 25 mL of CH_2Cl_2, washed with water (2×25 mL) and brine (25 mL), and dried over anhydr. $MgSO_4$. The solvent was removed (rotary evaporator) and the residue was crystallized from CH_2Cl_2–hexane to afford a light tan powder (0.33 g, quant.). An analytical sample of **7** was prepared by precipitation of a CH_2Cl_2 solution with hexane. Colorless crystals were collected and dried over P_2O_5 in a drying pistol overnight. Mp 132–133°C [lit.[21] mp 187–194°C, 198–200°C]; IR (KBr) ν: 3424, 1677, 1497, 1444, 1387, 1082, 744, 700, 612 cm^{-1}; ^{1}H NMR δ: 8.03 (1H, brs), 7.44–7.32 (5H, m), 3.92 (2H, s), 2.13 (3H, s) ppm; ^{13}C NMR δ: 174.92, 151.21, 132.53, 131.83, 129.31, 128.44, 127.85, 50.46, 14.48 ppm.

3.1.10. 2,18-Des-vinyl-2,18-bis-phenyl-bilirubin-IIIα (3).

In a 50 mL round bottomed flask, 3-methyl-4-phenyl-3-pyrrolin-2-one (**7**) (0.288 g, 1.57 mmol) and diformyl-dipyrrylmethane **14** (0.147 g, 0.393 mmol) were dissolved in 60 mL of 2-propanol and 0.32 mL of piperidine. The solution was heated at reflux overnight, during which time the product precipitated. The mixture was chilled in an ice bath, and the solids were collected by vacuum filtration then washed with water (2×10 mL). The yellow-orange solid was air dried to afford pure **3** (0.203 g, 75%). Mp 260–262°C; IR (KBr) ν: 3407, 2923, 1700, 1684, 1653, 1576, 1496, 1448, 1250, 667 cm^{-1}; ^{1}H NMR δ: 13.66 (3H, brs), 10.85 (2H, s), 9.36 (2H, s), 7.48–7.28 (10H, m), 6.22 (2H, s), 4.11 (2H, s), 3.04 (2H, ddd, J=13.5, 3.0, −14.5 Hz), 2.93 (2H, ddd, J=13.5, −15.8, 1.5 Hz), 2.82 (2H, ddd, J=3.0, −15.8, 4.5 Hz), 2.60 (2H, ddd, J=−14.5, 1.5, 4.5 Hz), 2.27 (6H, s), 2.20 (6H, s) ppm; ^{13}C NMR δ: 179.90, 173.58, 142.54, 134.13, 131.81, 129.44, 129.39, 128.57, 128.55, 127.75, 125.00, 124.64, 120.01, 102.35, 32.82, 22.52, 18.81, 11.02, 10.42 ppm. Anal. calcd for $C_{41}H_{40}N_4O_6$ (684.8): C, 71.91; H, 5.89; N, 8.18. Found: C, 72.22; H, 6.13; N, 8.12.

3.1.11. 3,17-Des-vinyl-3,17-bis-phenyl-bilirubin-XIIIα-dimethyl ester (5).

In a 50 mL round bottomed flask 3-methyl-4-phenyl-3-pyrrolin-2-one (**6**) (0.341 g, 1.97 mmol) and diformyldipyrrylmethane **13**[7,9,10] (0.198 g, 0.493 mmol) was dissolved in 10 mL of methanol and 2.0 mL of piperidine. The solution was heated at reflux overnight, during which time the product precipitated from the solution. The mixture was chilled in an ice bath, the solids collected by vacuum filtration, then washed with water (2×10 mL). The yellow-orange solid was air dried to afford pure dimethyl ester **5** (0.351 g, 56%). Mp 230–234°C (dec); IR (KBr) ν: 3338, 2918, 1738, 1658, 1633, 1464, 1361, 1252, 1165, 1019, 700 cm^{-1}; ^{1}H NMR δ: 11.27 (2H, s), 10.42 (2H, s), 7.36–7.11 (10H, m), 5.91 (2H, s), 4.18 (2H, s), 3.64 (6H, s), 2.85 (4H, t, J=7.4 Hz), 2.45 (4H, t, J=7.4 Hz), 1.95 (12H, s) ppm; ^{13}C NMR δ: 173.79, 173.69, 145.73, 132.84, 131.66, 130.02, 129.25, 128.38, 128.20, 124.75, 124.60, 124.32, 119.37, 104.57, 51.70, 35.68, 22.92, 20.30, 9.91, 8.73 ppm. Anal. calcd for $C_{43}H_{44}N_4O_6$ (712.8): C, 72.45; H, 6.22; N, 7.86. Calcd for $C_{43}H_{44}N_4O_6 \cdot 1/2H_2O$ (721.9): C, 71.55; H, 6.28; N, 7.76. Found: C, 71.97; H, 6.07; N, 7.65.

3.1.12. 2,17-Des-vinyl-2,17-bis-phenyl-bilirubin-IXα 12-monomethyl ester (4).

2,18-Des-vinyl-2,18-bis-phenyl-bilirubin-IIIα (**3**) (0.052 g, 0.073 mmol) and 3,17-des-vinyl-3,17-bis-phenyl-bilirubin-XIIIα dimethyl ester (**5**) (0.050 g, 0.073 mmol) were dissolved in DMSO (5 mL); then conc. HCl (0.50 mL) was added with stirring. The solution was stirred in the dark under a nitrogen atmosphere for 1 min and was poured into water (75 mL). The resulting solids were removed by centrifugation, and collected by vacuum filtration. The solids were washed with water (2×10 mL) and air dried to afford a 1:1:2 mixture of the two starting materials and the desired product, respectively. The rubins were separated and isolated by radial chromatography (eluent: from 100% CH_2Cl_2 to 5% methanol in CH_2Cl_2). The desired monomethyl ester (**4**) was obtained as a bright yellow-orange solid (0.048 g, 93%). Mp 280–282°C; IR (KBr) ν: 3334, 2918, 1658, 1626, 1456, 1362, 1249, 1166, 869, 700 cm^{-1}; ^{1}H NMR δ: 13.60 (1H, brs), 10.96 (1H, s), 9.39 (1H, s), 9.21 (1H, s), 8.56 (1H, s), 7.48–7.28 (10H, m), 6.12 (1H, s), 5.99 (1H, s), 4.04 (2H, s), 2.90–

2.77 (8H, m), 2.27 (3H, s), 2.20 (3H, s), 2.00 (3H, s), 1.93 (3H, s) ppm; ^{13}C NMR δ: 179.85, 176.30, 174.34, 171.18, 146.39, 142.15, 133.35, 132.33, 132.27, 131.86, 130.35, 129.78, 129.71, 129.60, 129.01, 128.70, 128.65, 128.43, 128.11, 127.60, 124.77, 124.70, 124.65, 123.07, 120.27, 118.96, 104.78, 99.55, 53.14, 34.07, 32.83, 22.52, 19.57, 18.99, 11.12, 10.57, 9.99, 9.08 ppm. Anal. calcd for $C_{42}H_{42}N_4O_6$ (698.8): C, 72.19; H, 6.06; N, 8.02. Calcd for $C_{42}H_{42}N_4O_6 \cdot H_2O$ (716.8): C, 70.37; H, 6.19; N, 7.82. Found: C, 70.70; H, 5.77; N, 7.57.

3.1.13. 2,17-Des-vinyl-2,17-bis-phenyl-bilirubin-IXα (1).

2,17-Des-vinyl-2,17-bis-phenyl-bilirubin-IXα 12-mono-methyl ester (4) (0.046 g, 0.068 mmol), disodium-EDTA (2.0 mg), and ascorbic acid (50.0 mg) were dissolved in 120 mL of methanol and 60 mL of 1 M aq. sodium hydroxide. The solution was stirred under argon at 40°C for 30 min. After acidification with acetic acid, the solution was extracted with CH_2Cl_2 (3×50 mL). The combined extracts were washed with water (150 mL) and brine (50 mL), and dried over anhydr. $MgSO_4$. The solvent was removed on a rotary evaporator and the residue purified by radial chromatography (eluent: CH_2Cl_2) to afford 1 as a pure orange-yellow product (0.025 g, 56%). Mp 315–316°C; IR (KBr) ν: 3408, 2912, 1693, 1681, 1573, 1440, 1404, 1249, 785 cm^{-1}; ^{1}H NMR δ: 13.74 (1H, s), 13.62 (1H, s), 10.92 (1H, s), 10.84 (1H, s), 9.35 (1H, s), 9.30 (1H, s), 7.48–7.28 (10H, m), 6.23(1H, s), 5.97 (1H, s), 4.10 (2H, s), 3.08–2.54 (8H, m), 2.27 (3H, s), 2.21 (3H, s), 2.02 (3H, s), 1.92 (3H, s) ppm; ^{13}C NMR δ: 179.88, 174.29, 173.57, 146.47, 142.52, 134.20, 133.79, 132.32, 131.81, 129.75, 129.45, 129.40, 128.83, 128.69, 128.66, 128.56, 127.75, 127.23, 124.98, 124.80, 124.63, 124.53, 120.01, 119.88, 104.60, 102.30, 32.85, 32.76, 22.53, 18.82, 18.78, 11.04, 10.43, 10.32, 9.06 ppm. Anal. calcd for $C_{41}H_{40}N_4O_6$ (684.8): C, 71.91; H, 5.89; N, 8.18. Found: C, 71.97; H, 5.91; N, 8.08.

3.2. Animal studies

Details of the experimental procedures used for studying the hepatic metabolism and biliary excretion of 1–3 in rats have been described in detail elsewhere.[19,22] Briefly, a femoral vein and the common bile duct were cannulated under ketamine anesthesia and a liposomal solution[7,10,19] containing phosphatidylcholine (1.5 g), cholesterol (62 mg), sodium cholate (12.95 g) and taurine (3.75 g) in 1 L of water was infused (2 mL/hr) through the femoral catheter to maintain hydration and ensure a steady bile flow rate (measured gravimetrically). Once the bile flow rate and body temperature (maintained with an infra-red heating lamp) had stabilized (~30–60 min), a solution containing 0.25 mg pigment in 1 mL rat serum was infused via the femoral vein as a bolus over a period of about 1 min. The infusate was prepared by dissolving the pigment in 0.1 mL DMSO, diluting this solution with 1 mL rat serum and microfuging to remove any undissolved or particulate material. Bile was collected in 20 µL aliquots from the tip of the bile duct cannula immediately before injection of pigment and at frequent intervals thereafter. The total length of the biliary cannula was 3 in., of which ~1.25 in. protruded to the outside through the skin. Collection of each bile sample took about 20 s. Immediately after collection, samples were flash frozen in dry-ice and stored at

−70°C in the dark until analyzed by HPLC. For HPLC, samples (20 µL) were mixed with 80 µL of ice-cold 0.1 M methanolic di-n-octylamine acetate (prepared by dissolving equimolar quantities of di-n-octylamine and acetic acid in methanol), microfuged for 30 s and 20 µL of the clear supernate was injected onto the column. Biliary excretion curves were derived by plotting HPLC peak areas, determined by integration, against time and are not corrected for small variations in bile flow-rate or differences in the extinction coefficients of the individual components. For hydrolysis of glucuronides with β-glucuronidase, bile (20 µL) was mixed with 40 µL of β-glucuronidase solution (prepared by adding 1 mL of water to one vial of bacterial β-glucuronidase on ice), the mixture incubated for 1 h at 37°C in the dark and then mixed vigorously with 140 µL of 0.1 M di-n-octylamine acetate in methanol. This mixture was microfuged for 30–60 s and an aliquot (20 µL) of the supernate was taken for HPLC. For base hydrolysis of glucuronides, bile (20 µL) was mixed with 1 M NaOH (10 µL). After 30 min at room temperature, 10 µL 1 M HCl was added followed, after mixing, by 160 µL of 0.1 M di-n-octylamine acetate in methanol. The mixture was vortexed, microfuged for 30–60 s and an aliquot (20 µL) of the supernate was taken for HPLC.

References

1. Bosma, P. J.; Seppen, J.; Goldhoorn, B.; Bakker, C.; Oude Elferink, R. P.; Chowdhury, N. R.; Chowdhury, N. R.; Jansen, P. L. *J. Biol. Chem.* **1994**, *269*, 17960–17964.
2. Coffman, B. L.; Green, M. D.; King, C. D.; Tephly, T. R. *Mol. Pharmacol.* **1995**, *47*, 1101–1105.
3. Owens, I. S.; Ritter, J. K.; Yeatman, M. T.; Chen, F. *J. Pharmacokin. Biopharma.* **1996**, *24*, 491–508.
4. Ramonas, L. M.; McDonagh, A. F.; Palma, L. A. *J. Pharmacol. Methods* **1981**, *5*, 149–164.
5. Bonnett, R.; Davies, J. E.; Hursthouse, M. B.; Sheldrick, G. M. *Proc. R. Soc. Lond., Ser. B* **1978**, *202*, 249–268.
6. Person, R. V.; Peterson, B. R.; Lightner, D. A. *J. Am. Chem. Soc.* **1994**, *116*, 42–59.
7. Brower, J. O.; McDonagh, A. F.; Lightner, D. A. *Tetrahedron* **2000**, *56*, 7869–7883.
8. Trull, F. R.; Rodríguez, M.; Lightner, D. A. *Synth. Commun.* **1993**, *23*, 2771–2783.
9. Mironov, A. F.; Evstigneeva, R. P.; Preobrazenskii, N. A. *J. Gen. Chem. USSR* **1965**, *35*, 1938–1943.
10. Chen, Q.; Huggins, M. T.; Lightner, D. A.; Norona, W.; McDonagh, A. F. *J. Am. Chem. Soc.* **1999**, *121*, 9253–9264. In this reference may be found a simplified high yield TosMIC synthesis.
11. Kohori, K.; Kinoshita, H.; Inomata, K. *Chem. Lett.* **1995**, 799–800.
12. Kaplan, D.; Navon, G. *Isrl. J. Chem.* **1983**, *23*, 177–186.

13. Molecular mechanics calculations and molecular modeling were carried out on an SGI Octane workstation using version 6.6 of Sybyl (Tripos Assoc., St Louis, MO) as described in Ref. 6. The ball and stick drawings were created from the atomic coordinates of the molecular dynamics structures using Müller and Falk's Ball and Stick program for the Macintosh.

14. Lightner, D. A.; Gawronski, J. K.; Wijekoon, W. M. D. *J. Am. Chem. Soc.* **1987**, *109*, 6354–6362.

15. Lightner, D. A.; An, J. Y.; Pu, Y. M. *Arch. Biochem. Biophys.* **1988**, *262*, 543–559.

16. Harada, N.; Nakanishi, K. *Circular Dichroic Spectroscopy—Exciton Coupling in Organic Stereochemistry*; University Science Books: Mill Valley, CA, 1983.

17. Pu, Y.-M.; McDonagh, A. F.; Lightner, D. A. *J. Am. Chem. Soc.* **1993**, *115*, 377–380.

18. Lightner, D. A.; Wijekoon, W. M. D.; Zhang, M.-H. *J. Biol. Chem.* **1988**, *263*, 16669–16676.

19. McDonagh, A. F.; Lightner, D. A. *Cell. Mol. Biol.* **1994**, *40*, 965–974.

20. Eby, J. M.; Moore, J. A. *J. Org. Chem.* **1967**, *32*, 1346–1353.

21. Wineholt, R. L.; Wyss, E.; Moore, J. A. *J. Org. Chem.* **1966**, *31*, 48–52.

22. McDonagh, A. F. *The Porphyrins*; Dolphin, D., Ed.; Academic Press: New York, 1979; Vol. 6, pp 293–491.